International Journal of Nanoelectronics and Materials
IJNeaM
ISSN 1985-5761 | E-ISSN 2232-1535

Fabrication and Characterization of Nanostructured Tin doped Indium Oxide Coatings by the Instrument of Spray Pyrolysis

Salam Amir Yousif

Department of Physics, College of Education, Mustansiriyah University, Baghdad – Iraq
e-mail: salammomica@uomustansiriyah.edu.iq

Received 8 June 2023, Revised 20 August 2023, Accepted 14 November 2023

ABSTRACT

Nanostructured indium tin oxide (ITO) coating is one of the transparent conductive oxides (TCO) materials utilized as a transparent electrode. Due to its high demand in various applications like liquid crystal displays, touch screens, light emitting devices, and solar cells, ITO coatings have garnered significant research attention, owing to their excellent properties of high visible light transmittance and low resistance. Nanostructured coating of tin -doped Indium Oxide (ITO) was fabricated on glass slides utilizing the instrument of chemical spray pyrolysis (CSP), with varying levels of Sn-doping at 0, 3, 6, and 9 wt%. The effect of tin content on the many physical characteristics of the resulting coatings has been examined. The analysis of x-ray diffraction (XRD) displayed the characteristic In_2O_3 orientations. The coatings have a polycrystalline cubic lattice structure along (400) as the preferred growth direction. Morphological measurements indicate that the samples possess a highly uniform surface and the grain size for the ITO samples is ≤ 100 nm displaying a nanostructure for all samples. The optical transmittance was measured over 75% for coating with tin content equal to 0wt%, while the transmittance of the Sn-doped films can range from 78% to 84% at 700 nm and the values of the direct bandgap (E_g) were measured as 3.6, 3.65, 3.675, and 3.7eV for Sn doping 0, 3, 6, and 9 wt% respectively. In the visible area, the nanostructured ITO coatings exhibit elevated values of transmittance which makes them suitable for various optoelectronic applications such as window materials in solar cells. The results indicate a desirable reduction in the electrical resistivity with rising the number of carriers per unit volume and mobility with increasing tin content in the samples. The minimum electrical resistivity (0.1459 Ω . cm) and maximum carrier concentration (2.128×10^{18} cm^{-3}) were achieved for ITO coating with tin content equal to 9wt%. The incorporation of Sn dopant significantly changes the overall electrical properties of indium oxide films, this is favorable for transparent conducting oxide.

Keywords: *Electrical characteristics, ITO coatings, Spray pyrolysis, Morphology, Tin doping, Nanostructure*

1. INTRODUCTION

Transparent Conducting Oxide (TCO) coatings, which possess both transparency and conductivity, have sparked great interest in their potential applications in solar energy conversion, sensors, and various electrode uses. ITO coating is one of the transparent and conducting oxide substances that is commonly known for its n-type behavior. Nanostructured ITO coatings are utilized as a transparent electrode. Due to its high demand in various applications like liquid crystal displays, touch screens, light emitting devices, and solar cells, ITO coatings have garnered significant research attention, owing to their excellent properties of high visible light transmittance and low resistance. In the In_2O_3 crystal lattice, tin acts as a positive ions impurities that occupy the substitute sites of indium to form a bond with interstitial oxygen. ITO is widely used in optoelectronic devices because it has high optical transmittance, low electrical resistivity, and broad bandgap ($> 3.5eV$). Applications of ITO include solar cells [1], visual display (LCD)[2], sensors of gases [3] and antireflection coatings [4]. Different techniques are used to fabricate ITO thin films, such as magnetron sputtering [5-7], sol-gel processes [8-10], thermal evaporation [11], pulsed laser deposition [12,13], chemical vapor deposition [14,15], and the spray pyrolysis technique [16-21].

In 2016, Thirumoorthi and Prakash [22] used the instrument of jet nebulizer spray pyrolysis to produce ITO coatings with varying Sn content. The resulting films were found to exhibit n-type conductivity with low resistivity ($3.9 \times 10^{-4} \Omega.cm$) and high carrier concentrations ($6.1 \times 10^{20} cm^{-3}$), as confirmed by Hall effect measurements. The objective of this research is to investigate the impact of tin doping on the structural, morphological, optical, and electrical characteristics of nanostructured ITO coatings created by the instrument of chemical spray pyrolysis for use in optoelectronic implementations.

2. PROCEDURE

Nanostructured ITO coatings were fabricated using the instrument of CSP with varying Sn-doping on a glass substrate at a hot plate temperature of around 450°C, as illustrated in Figure 1. To obtain a homogeneous and clear solution, Indium Chloride InCl3 (purity of 98%, Thomas Baker, India), Stannic Chloride SnCl4.5H2O (purity of 99%,

Chemical Point, Germany), and 100 ml of distilled water were thoroughly added to form a solution of 0.05 $(mole/liter)$, to which one or two drops of HCl acid was put to increase the solubility. Prior to deposition, the distilled water was used to wash the slides in an ultrasonic bath for (10-15) min, followed by cleaning the slides using an amount of alcohol and acetone solutions. An Air blower was used to dry the slides. X-ray Diffraction (XRD) technique was utilized to study the structural characteristics of nanostructured ITO Thin films, specifically the Shimadzu 6000. An Instrument of SPM AA3000 Angstrom Advanced Inc. was utilized to study the topographic characteristics of nanostructured ITO thin films. A Spectrophotometer type (Shimadzu UV-1650 PC) was utilized to study the optical characteristics of nanostructured ITO thin films by analyzing the spectra of transmittance and the spectra of absorbance as a wavelength difference from 300 to 900nm.

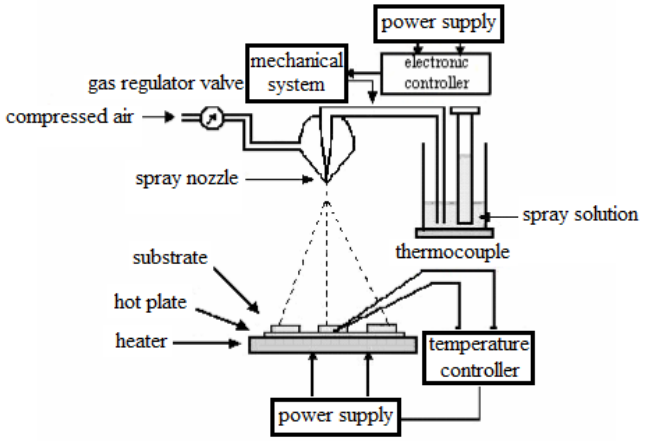

Figure 1 Instrument of CSP.

3. RESULTS AND DISCUSSION

3.1 Structural characteristics

The X-ray diffraction technique was used to determine the crystal structure of deposited nanostructured ITO thin films. The films were deposited onto a glass substrate at a temperature of (450 ℃) with varying levels of Sn doping, and the resulting XRD patterns were recorded in the range of (15-70) degrees 2θ. All diffractograms displayed the characteristic In_2O_3 orientations, and the observed d-values were compared to standard values from the JCPDS (card 06-0416 In_2O_3,cubic). The matching of the observed and standard d-values confirmed that the films had a polycrystalline cubic structure. The X-ray diffraction spectra showed that all ITO films with different Sn doping levels had a preferred orientation of (400), with the (222) peak being the strongest in all the films. Other peaks, such as (211), (431), (440), and (622), were also detected but with lower intensities. Figure 1 depicts the XRD patterns of spray-deposited ITO thin films with different Sn doping levels of 0, 3, 6, and 9 wt%. The intensity of the (222) peak increased with increasing tin content, while the intensity of the (400) peak decreased. This decrease in (400) peak intensity may be due to a change in growth rate, which results in thinner ITO films. Table 1 lists the structural characteristics of nanostructured ITO thin films for different Sn-doping corresponding to the (400) as preferred peak orientation.

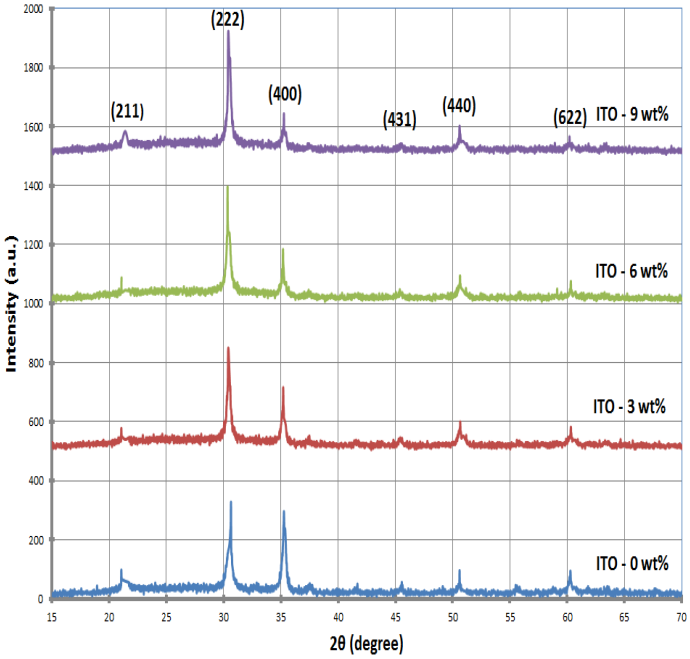

Figure 2. X-ray diffraction peaks of nanostructured ITO coatings as a function of tin content.

Lattice distance (a) of nanostructured ITO coatings was calculated using the inter planer spacing (d) for (400) peak as preferred growth orientation using the following equation:

$$d = \frac{a}{\sqrt{h^2+k^2+l^2}} \qquad (1)$$

Furthermore, the Debye - Scherrer formula [23] was used to calculate crystallite size:

$$crystallite\ size\ (D) = \frac{0.9 \times \lambda}{\beta \times cos\theta} \qquad (2)$$

The amount of defects in the nanostructured ITO crystal can be represented by dislocation density (δ***)*** is calculated using the following equation [24]:

$$\delta = \frac{1}{D^2} \qquad (3)$$

The stretching or compression in the nanostructured ITO crystal lattice leads to the deviation in the distance between the atoms from the standard value and is represented by the strain which is calculated using the following equation[24]:

$$\varepsilon_\circ = \frac{\beta\ cos\theta}{4} \qquad (4)$$

The Texture coefficient (TC) of nanostructured ITO coatings describe the preferred growth orientation is calculated using the following equation [25]:

$$T_c(hkl) = \frac{I(hkl)/I_0(hkl)}{N_r^{-1}\sum I(hkl)/I_0(hkl)} \qquad (5)$$

Table 1 Structural characteristics of nanostructured ITO coatings

Sn-doping wt%	0	3	6	9
Interplaner spacing d (Å)	2.534	2.536	2.538	2.535
2θ (deg)	35.39	35.36	35.32	35.36
$FWHM$ (deg)	0.354	0.366	0.347	0.351
Crystallite size (nm)	23.5	22.7	23.9	23.7
Dislocation density $\delta\,(line/m^2) \times 10^{15}$	1.81	1.94	1.75	1.78
Strain $\varepsilon_0 \times 10^{-3}$	1.47	1.52	1.44	1.46
Lattice parameter a (Å)	10.13	10.14	10.15	10.14
Texture coefficient (T_C)	2.1730	1.6736	1.7304	1.3328

3.2 Topography characteristics

Figure 3 illustrates three-dimensional atomic force microscopy (AFM) images of nanostructured ITO samples with varying levels of tin doping. Table 2 demonstrates that increasing the tin doping causes variations in the AFM parameters. As the tin content rises, the root mean square (RMS) roughness of the nanostructured ITO thin films increases from 2 to 3.56 nm due to a rise in vacancy defects and the rearrangement of atoms. Morphological measurements indicate that the samples possess a highly uniform surface. The size of grains (D) for the nanostructured ITO thin films are 77, 95, 96, and 100 nm for tin doping of 0, 3, 6, and 9 wt%, in the same order, displaying a nanostructure for all samples. The AFM study reveals a strong dependence between the grain size, surface roughness, and the concentration of tin doping in the ITO samples.

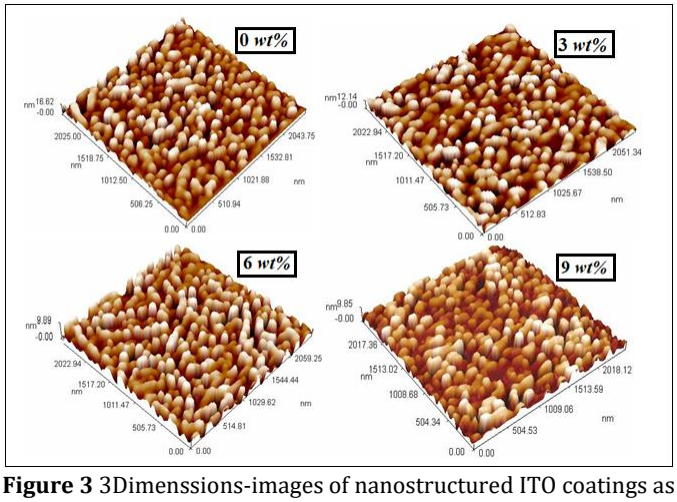

Figure 3 3Dimenssions-images of nanostructured ITO coatings as a function of tin content.

Figure 4 shows the grain size distribution of ITO coatings fabricated on glass slides by the instrument of CSP under ambient atmosphere at a temperature of 450°C . It can be observed from these figures that the addition of tin atoms as a dopant in the films leads to a more homogeneous distribution of the grains. The homogeneity of grain size distribution reaches its highest level when the Sn doping concentration is 9wt%. In other words, the granularity distribution of ITO grains becomes increasingly homogeneous, when the tin content in the ITO coatings rises.

Table 2 Topographic characteristics of nanostructured ITO coatings for different Sn-doping.

Sn – Doping wt%	RMS roughness (nm)	Size of grains (nm)
0	2	77
3	2.3	95
6	2.7	96
9	3.5	100

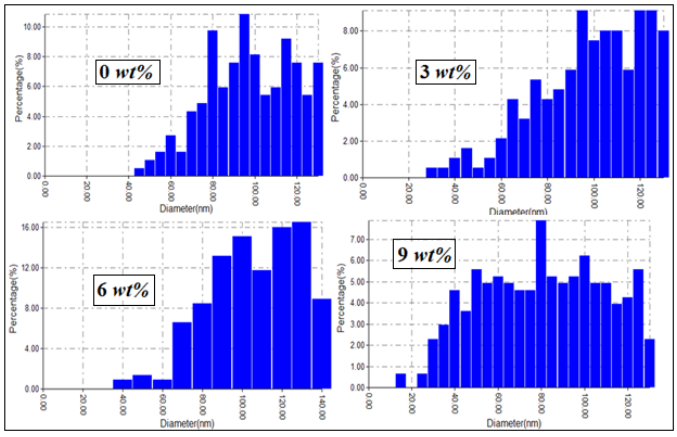

Figure 4 Granularity distribution of nanostructured ITO coatings as a function of tin content.

3.3 Optical characteristics

Figure 5 displays the transmittance of nanostructured ITO coatings prepared at various doping concentrations, which were examined at (27 °C), as a function of wavelength. The absorption edge of nanostructured ITO coatings lies in the ultraviolet region with high optical transparency found for high values of wavelength range. The transmittance of nanostructured ITO coatings, as shown in figure 5, increases with increasing the value of tin content in the coatings due to improvements in the crystalline structure. It was observed that the minimum value of optical transmittance measured at room temperature for tin content equal to 0 wt% is over 75%, while the transmittance of the Sn-doped films can range from 78% to 84% at a wavelength equal to 700nm. These findings can be attributed to the decrease in coatings layer thickness which leads to a decrease in the amount of light that scatters from the nanostructured ITO coatings.

The introduction of doping led to the gradual crystallization of the nanostructured ITO thin films, resulting in improved carrier density and mobility. As a result, surface resistance was reduced. The increased carrier density also led to a decrease in the presence of black indium oxide molecules, thereby enhancing the light transmission in the wavelength ranging from (400-700) nm. Figure 6 illustrates the absorption coefficient of the nanostructured ITO coatings, showing a decrease in absorption coefficient with increasing Sn doping.

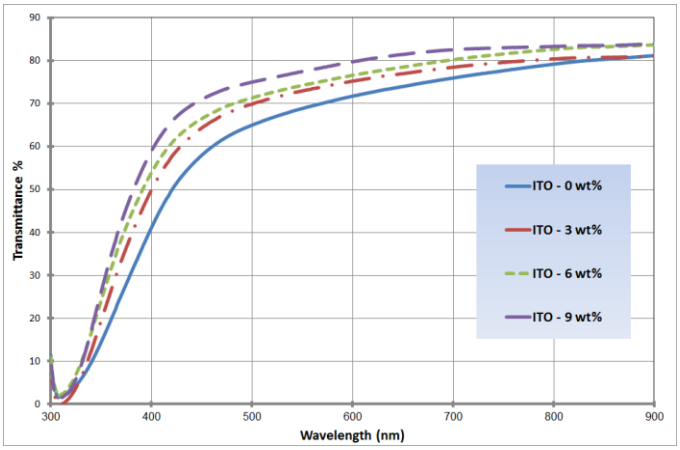

Figure 5 UV-VIS transmittance spectra of nanostructured ITO coatings as a function of tin content.

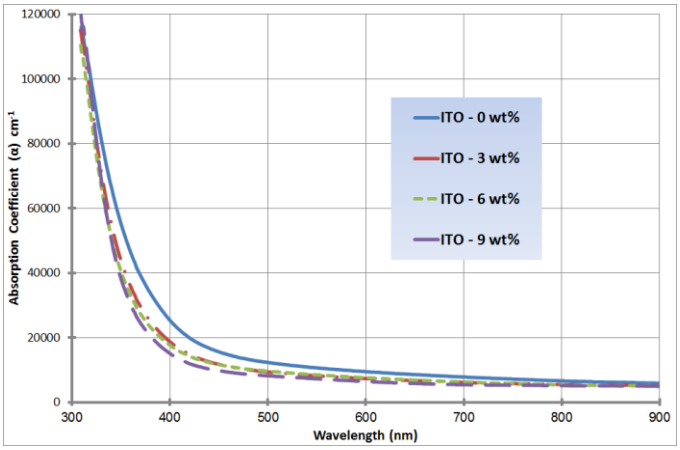

Figure 6 Absorption Coefficient of nanostructured ITO coatings as a function of tin content.

The optical bandgap energy (E_g) of nanostructured ITO coatings can be calculated using the equation [26]:

$$A h\gamma = A(h\gamma - E_g)^x \qquad (7)$$

For pure and doped films at 3, 6, and 9wt%, the values of the direct bandgap were measured as 3.6, 3.65, 3.675, and 3.7eV, in the same order. Figure 7 illustrates that the energy bandgap of the nanostructured ITO coatings increases with higher tin content, which is consistent with previous research [22].

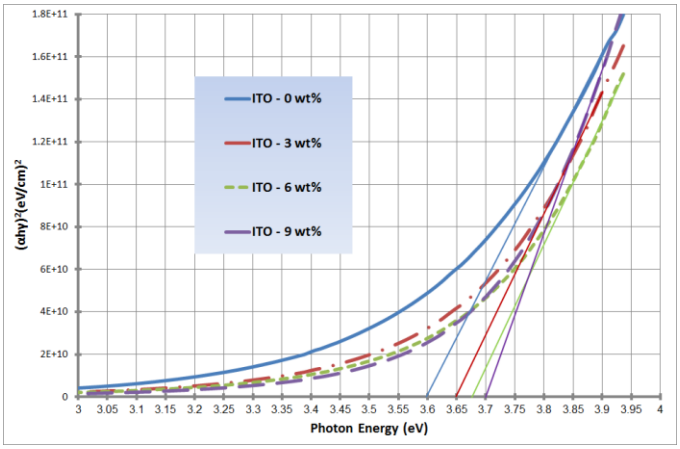

Figure 7 energy bandgap of nanostructured ITO coatings as a function of tin content.

The absorption edge is shifted towards higher frequencies due to the increase of energy bandgap of nanostructured ITO coatings as depicted in Figure 5. From the introduction of the Burstein-Moss formula, the shift of the Fermi level towards the conduction band causes the larger of the energy bandgap, subsequently increasing the number of carriers per unit volume. The shift of absorption edge towards the high frequencies leads to the increase of the size of grains in nanostructured ITO thin films, which is consistent with the research [27].

3.4 Electrical characteristics

Figures (8 – 10) illustrate the electrical parameters of nanostructured ITO coatings that were prepared with varying Sn doping. The results indicate a desirable decrease in resistivity and an increase in carrier concentration and mobility with increasing Sn doping, This is favorable for the materials that have high conductivity and high transparency. The findings indicate that the prepared ITO coatings possess highly degenerate n-type conductivity. The increase in carrier concentration is attributed to the valence difference between Sn^{4+} and In^{3+} ions, resulting in the generation of an extra free carrier per atomic substitution and leading to a decrease in resistivity. The incorporation of Sn dopant significantly changes the overall electrical properties of indium oxide films. The minimum electrical resistivity $(0.1459\,\Omega\,.cm)$ and maximum carrier concentration $(2.128 \times 10^{18}\,cm^{-3})$ were achieved for tin content equal to 9wt%, which is consistent with previous literatures [22, 28]. The mobility of nanostructured ITO coatings increases with increasing tin content is explained by the decrease of grain boundary scattering, and the movement of electrons of the ultrathin coating is entirely related to the nanostructure and doping concentration.

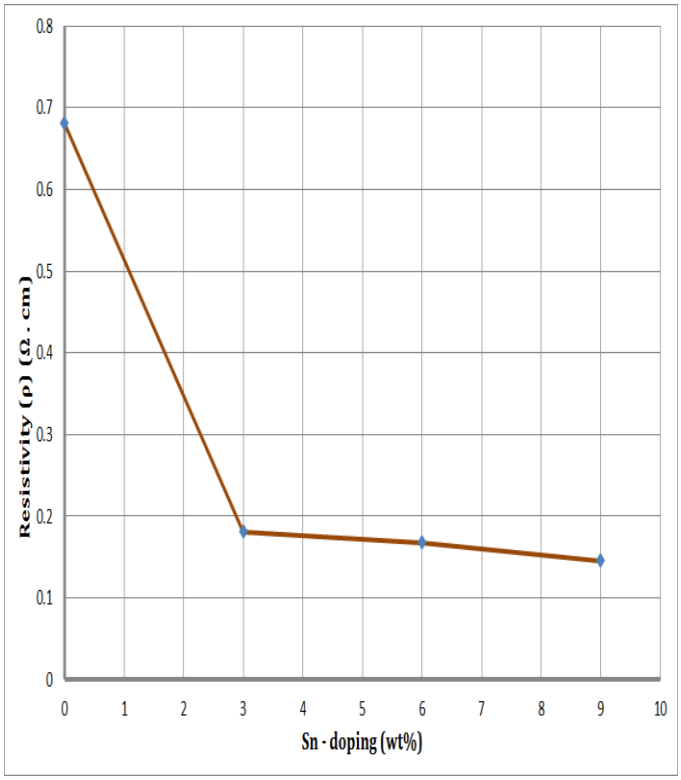

Figure 8 The Resistivity of nanostructured ITO coatings as a function of tin content.

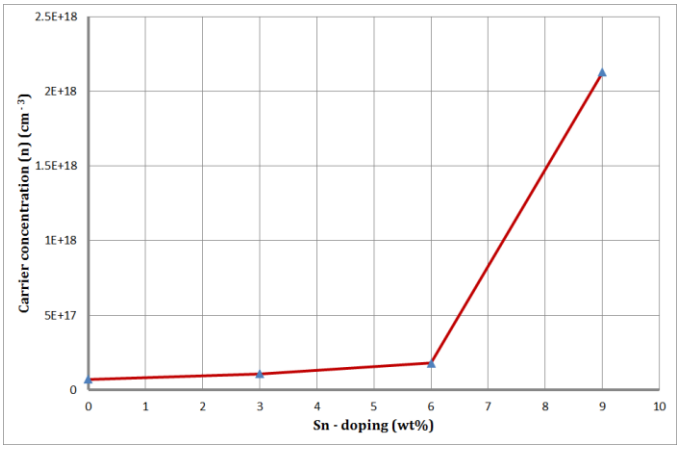

Figure 9 Carrier concentration of nanostructured ITO coatings as a function of tin content.

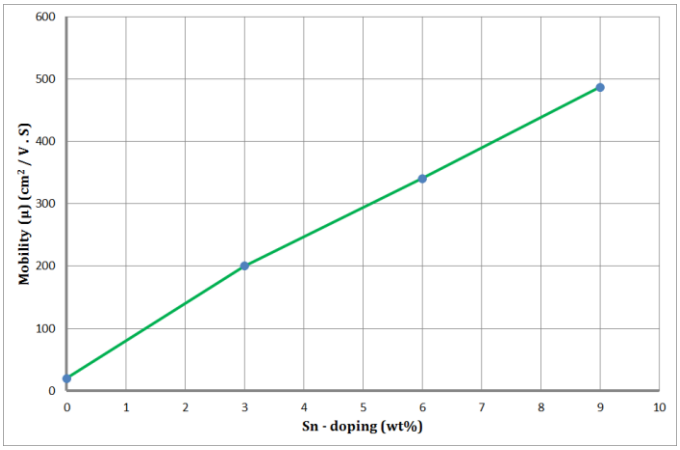

Figure 10 Mobility of nanostructured ITO coatings as a function of tin content.

4. CONCLUSIONS

Successful preparation of nanostructured ITO coatings with varying levels of tin content on glass slides was achieved by utilizing the instrument of CSP. The effects of tin content on the crystal structure, morphological, optical, and electrical characteristics of the ITO coatings were demonstrated. Raising the Sn doping in this study holds significance in enhancing the activity of nanostructured ITO coatings in optoelectronic instruments when utilized as electrodes that exhibit both transparency and conductivity. This improvement is achieved by increasing the size of grains and the transmittance of nanostructured ITO thin films in the visible area, thereby enhancing the electrical conductivity. ITO coatings exhibit a nanostructure, and with the increase in tin content, the grain size of the nanostructured ITO coatings also increases. Notably, in the visible area, the nanostructured ITO coatings exhibit elevated values of transmittance which makes them suitable for various optoelectronic applications such as window materials in solar cells. Additionally, the increase in tin content results in higher grossness, improved transmittance, and increased values of the energy bandgap for the samples. The incorporation of Sn dopant significantly changes the overall electrical properties of indium oxide films, this is favorable for transparent conducting oxide. This research illustrated that the optical transmittance and electrical conductivity of nanostructured ITO coatings are highly affected by the tin doping processes, this in turn, leads to improve optical and electrical properties of nanostructured ITO coatings in optoelectronic applications such as solar cells, touch screens and liquid crystal displays.

ACKNOWLEDGEMENT

The author would like to express his sincere gratitude to Mustansiriyah University, located in Baghdad, Iraq (www.uomustansiriyah.edu.iq), for their invaluable assistance in this work.

REFERENCES

[1] D. Gebeyehu, C. J. Brabec, N. S. Sariciftci, D. Vangeneugden, R. Kiebooms, D. Vanderzande, F. Kienberger, and H. Schindler, "Hybrid solar cells based on dye-sensitized nanoporous TiO2 electrodes and conjugated polymers as hole transport materials," *Synthetic Metals*, vol. 125, no. 3, pp. 279-287, 2001.

[2] J. C. Manifacier, "Thin metallic oxides as transparent conductors," *Thin Solid Films*, vol. 90, no. 3, pp. 297-308, 1982.

[3] G. Neri, A. Bonavita, G. Micali, G. Rizzo, E. Callone, and G. Carturan, "Resistive CO gas sensors based on In2O3 and InSnOx nanopowders synthesized via starch-aided sol–gel process for automotive applications," *Sensors and Actuators B: Chemical*, vol. 132, no. 1, pp. 224-233, 2008.

[4] S. A. Yousif, H. G. Rashid, K. A. Mishjil, and N. F. Habubi, "Design and Preparation of Low Absorbing Antireflection Coatings Using Chemical Spray Pyrolysis," *International Journal of Nanoelectronics and Materials*, vol. 11, no. 4, pp. 449-460, 2018.

[5] J. H. Park, C. Buurma, S. Sivananthan, R. Kodama, W. Gao, and T. A. Gessert, "The effect of post-annealing on Indium Tin Oxide thin films by magnetron sputtering method," *Applied Surface Science*, vol. 307, pp. 288-392, 2014.

[6] L. Dong, G. Zhu, H. Xu, X. Jiang, X. Zhang, Y. Zhao, D. Yan, L. Yuan, and A. Yu, "Fabrication of Nanopillar Crystalline ITO Thin Films with High Transmittance and IR Reflectance by RF Magnetron Sputtering," *Materials*, vol. 12, no. 6, pp. 958-968, 2019.

[7] K. C. Heo, Y. K. Sohn, and J. S. Gwag, "Effects of an additional magnetic field in ITO thin film deposition by magnetron sputtering," *Ceramics International*, vol. 41, no. 1, pp. 617-621, 2015.

[8] Y. Wang, J. Liu, X. Wu, and B. Yang, "Adhesion enhancement of indium tin oxide (ITO) coated quartz optical fibers," *Applied Surface Science*, vol. 308, pp. 341-346, 2014.

[9] M. T. Kesim and C. Durucan, "Indium tin oxide thin films elaborated by sol-gel routes: The effect of oxalic acid addition on optoelectronic properties," *Thin Solid Films*, vol. 545, pp. 56-63, 2013.

[10] L. Korosi, S. Korosi, and I. Dekany, "Preparation of transparent conductive indium tin oxide thin films from nanocrystalline indium tin hydroxide by dip-coating method," *Thin Solid Films*, vol. 519, no. 10, pp. 3113-3118, 2011.

[11] K.-Y. Pan, L.-D. Lin, L.-W. Chang, and H. C. Shih, "Studies on the optoelectronic properties of the thermally evaporated tin-doped indium oxide nanostructures," *Applied Surface Science*, vol. 273, pp. 12-18, 2013.

[12] J. B. Choi, J. H. Kim, K. A. Jeon, and S. Y. Lee, "Properties of ITO films on glass fabricated by pulsed laser deposition," *Materials Science and Engineering*, vol. 102, issues 1-3, pp. 376-379, 2003.

[13] J. M. Dekkers, G. Rijnders, and D. H. A. Blank, "Role of Sn doping in In2O3 thin films on polymer substrates by pulsed-laser deposition at room temperature," *Applied Physics Letters*, vol. 88, issue 15, pp. 151908-151910, 2006.

[14] Y. C. Park, Y. S. Kim, H. K. Seo, S. G. Ansari, and H. S. Shin, "ITO thin films deposited at different oxygen flow rates on Si(100) using the PEMOCVD method," *Surface and Coatings Technology*, vol. 161, issue 1, pp. 62-69, 2002.

[15] Y. S. Kim, Y. C. Park, S. G. Ansari, B. S. Lee, and H. S. Shin, "Effect of substrate temperature on the bonded states of indium tin oxide thin films deposited by plasma enhanced chemical vapor deposition," *Thin Solid Films*, vol. 426, issues 1-2, pp. 124-131, 2003.

[16] G. G. Untila, T. N. Kost, and A. B. Chebotareva, "Fluorine- and tin-doped indium oxide films grown by ultrasonic spray pyrolysis: Characterization and application in bifacial silicon concentrator solar cells," *Solar Energy*, vol. 159, issue 1, pp. 173-185, 2018.

[17] R. Rana, J. Chakraborty, S. K. Tripathi, and M. Nasim, "Study of conducting ITO thin film deposition on flexible polyimide substrate using spray pyrolysis," *Journal of Nanostructure in Chemistry*, vol. 6, pp. 65-74, 2016.

[18] K. Navya, S. P. Bharath, K. V. Bangera, and G. K. Shivakumar, "Effect of indium content on the characteristics of indium tin oxide thin films," *Materials Research Express*, vol. 5, issue 9, 096410, 2018.

[19] L. Zhang, J. Lan, J. Yang, S. Guo, J. Peng, L. Zhang, S. Tian, S. Ju, W. Xie (2017). Study on the physical properties of indium tin oxide thin films deposited by microwave-assisted spray pyrolysis, *Journal of Alloys and Compounds*, Vol. 728, Issue 6, 1338-1345.

[20] S. A. Yousif (2023). Preparation and Characterization of Nanostructured ITO Thin Films by Spray Pyrolysis Technique: Dependence on Annealing Temperature, *International Journal of Nanoelectronics and Materials*, Vol. 16, Issue 2, 33-42.

[21] K. Ravichandran and K. Thirumurugan (2014). Type Inversion and Certain Physical Properties of Spray Pyrolysed SnO2:Al Films for Novel Transparent Electronics Applications*, Journal of Materials Science and Technology*, Vol. 30, Issue 2, 97-102.

[22] M. Thirumoorthi & J. Thomas Joseph Prakash (2016). Structural, optical and electrical properties of indium tin oxide ultra-thin film prepared by jet nebulizer spray pyrolysis technique, *Journal of Asian Ceramic Societies*, Vol. 4, Issue 1, 124-132.

[23] L. Dong, G. Zhu, H. Xu, X. Jiang, X. Zhang, Y. Zhao, D. Yan, L. Yuan and A. Yu (2019). Fabrication of Nanopillar Crystalline ITO Thin Films with High Transmittance and IR Reflectance by RF Magnetron Sputtering, *Materials*, Vol. 12, Issue 6, 958.

[24] M. Thirumoorthi and J. Thomas Joseph Prakash (2015). Structural, morphological characteristics and optical properties of Y doped ZnO thin films by sol-gel spin coating method, Super lattices and Microstructures, Vol. 85, 237-247.

[25] J. Hotovy, J. Hupkes, W. Bottler, E. Marins, L. Spiess, T. Kups, V. Smirnov, I. Hotovy, J. Kovac (2013). Sputtered ITO for application in thin-film silicon solar cells: Relationship between structural and electrical properties, *Applied Surface Science*, Vol. 269, 81-87.

[26] R. Chandramohan, T. A. Vijayan, S. Arumugam , H. B. Ramalingam, V. Dhanasekaran, K. Sundaram, T. Mahalingam (2011). Effect of heat treatment on microstructural and optical properties of CBD grown Al-doped ZnO thin films, *Material Science and Engineering* B, Vol. 176, Issue 2, 152-156.